Published in final edited form as:
*Cell Metab*. 2008 March ; 7(3): 205–214.

# Transferrin receptor modulates Hfe-dependent regulation of hepcidin expression

**Paul J. Schmidt**[1], **Paul T. Toran**[1], **Anthony M. Giannetti**[3,4], **Pamela J. Bjorkman**[3], and **Nancy C. Andrews**[1,2,5,*]

1*Division of Hematology/Oncology, Children's Hospital Boston; the Department of Pediatric Oncology, Dana-Farber Cancer Institute, Boston, MA 02115 USA*

2*Department of Pediatrics, Harvard Medical School, Boston, MA 02115 USA*

3*Division of Biology, California Institute of Technology, Pasadena CA 91125 USA*

5*Departments of Pharmacology & Cancer Biology and Pediatrics, Duke University School of Medicine, Durham, NC 27710*

## Summary

Hemochromatosis is caused by mutations in HFE, a protein that competes with transferrin (TF) for binding to the transferrin receptor (TFR1). We developed mutant mouse strains to gain insight into the role of the Hfe/Tfr1 complex in regulating iron homeostasis. We introduced mutations into a ubiquitously expressed *Tfr1* transgene or the endogenous *Tfr1* locus to promote or prevent the Hfe/Tfr1 interaction. Under conditions favoring a constitutive Hfe/Tfr1 interaction, mice developed iron overload attributable to inappropriately low expression of the hormone hepcidin. In contrast, mice carrying a mutation that interferes with the Hfe/Tfr1 interaction developed iron deficiency associated with inappropriately high hepcidin expression. High-level expression of a liver-specific *Hfe* transgene in $Hfe^{-/-}$ mice was also associated with increased hepcidin production and iron deficiency. Together, these models suggest that Hfe induces hepcidin expression when it is not in complex with Tfr1.

## Introduction

Hemochromatosis is a prevalent iron overload disease caused by a chronic increase in intestinal absorption of dietary iron. Most patients are homozygous for a C282Y mutation in *HFE*, a gene that encodes an atypical major histocompatibility class I-like molecule. Mice carrying homozygous mutations disrupting the *Hfe* gene ($Hfe^{-/-}$ and $Hfe^{C282Y/C282Y}$) have phenotypes that are very similar to human hemochromatosis (Ajioka et al., 2002; Levy et al., 1999b).

Although HFE is inferred to play a role in the regulation of intestinal iron absorption, its molecular function remains uncertain. HFE forms protein complexes with TFR1 and its liver-specific homolog, transferrin receptor 2 (TFR2) (Feder et al., 1998; Goswami and Andrews, 2006; Parkkila et al., 1997; Waheed et al., 1999). Iron-loaded transferrin (Fe-TF) can displace HFE from TFR1, because TF and HFE compete for overlapping binding sites on TFR1 (Bennett

*Address correspondence to: Nancy C. Andrews, M.D., Ph.D., Dean, Duke University School of Medicine, Rm. 125 Davison, Duke South, Green Zone, Durham, NC 27710, Phone: 919 684 2455, Email: nancy.andrews@duke.edu
4Current address: High Throughput Screening Group, Roche Palo Alto LLC, Palo Alto, CA 94304 USA

et al., 2000; Giannetti and Bjorkman, 2004; Lebron et al., 1998; Lebron and Bjorkman, 1999). Fe-TF also induces an increase in TFR2 protein stability (Johnson and Enns, 2004; Robb and Wessling-Resnick, 2004).

Initially, prevailing models postulated that HFE altered cellular uptake of iron through the TF cycle, thus programming intestinal absorptive cells to increase iron uptake. However, mice with duodenal-specific ablation of *Hfe* were reported to have no disruption of iron metabolism (Spasic et al., 2007). Expression of the iron-regulatory hormone hepcidin was shown to be inappropriately low in patients with HFE hemochromatosis and in $Hfe^{-/-}$ mice (Bridle et al., 2003a; Muckenthaler et al., 2003; Nicolas et al., 2003). Forced expression of a hepcidin transgene corrected the hemochromatosis phenotype in $Hfe^{-/-}$ mice, consistent with the interpretation that the primary role of Hfe is to control hepcidin expression (Nicolas et al., 2003). Hepcidin is produced by hepatocytes, which express more HFE than other cell types in the liver (Zhang et al., 2004). Furthermore, HFE hemochromatosis patients who have undergone orthotopic liver transplantation do not demonstrate re-accumulation of excess liver iron or markedly increased serum iron post-transplantation (Bralet et al., 2004). These observations refocused attention on HFE in hepatocytes, suggesting that the liver is the physiologically important site of the HFE/TFR1 and HFE/TFR2 interactions.

Hepcidin modulates iron homeostasis by binding to the iron exporter ferroportin at the cell surface, triggering ferroportin internalization and degradation (Nemeth et al., 2004b). Hepcidin-mediated inactivation of ferroportin on intestinal epithelial cells and macrophages apparently leads to decreased dietary iron absorption and accumulation of iron within the macrophage iron-recycling compartment (Donovan et al., 2005). In HFE hemochromatosis, production of hepcidin is inappropriately low for overall body iron status. Consequently, ferroportin activity is not attenuated, leading to increased iron absorption, increased return of macrophage iron to the circulation and deposition of surplus iron in parenchymal cells of target organs.

Hepcidin production is modulated in response to several physiological conditions. It increases in iron overload and decreases in iron deficiency (Pigeon et al., 2001; Weinstein et al., 2002). The occupancy of serum TF with iron has long been thought to play a role in communicating information about body iron stores (Cavill et al., 1975; Taylor and Gatenby, 1966). TF occupancy reflects the balance of iron entering the serum (from intestinal absorption, macrophage iron release, hepatic iron mobilization) and iron leaving the serum (primarily for utilization in erythropoiesis). TFR1 has much higher affinity for Fe-TF than for apo-TF (Aisen and Listowsky, 1980), suggesting that competition between HFE and TF for TFR1 binding might be modulated by TF occupancy with iron. Furthermore, the fact that TFR2 expression is induced by Fe-TF suggests that the HFE/TFR2 interaction may also be altered by TF saturation. We hypothesized that the purposes of the HFE/TFR1 and HFE/TFR2 interactions might, therefore, be to regulate hepcidin expression in response to body iron status. The HFE/TFR1 interaction is the subject of this report.

We generated three mutant mouse strains to interrogate the Hfe/Tfr1 interaction *in vivo*. First, we engineered a ubiquitously expressed *Tfr1* transgene carrying a missense mutation (R654A) that prevents Tf binding but does not affect interaction of Tfr1 and Hfe. These mice should have constitutive interaction of Hfe with Tfr1. Second, we introduced a missense mutation (L622A) into the endogenous *Tfr1* locus that renders Tfr1 unable to interact with Hfe, but has no major effect on Tf binding. Mice homozygous for this allele should have an insignificant decrease in the affinity of Tfr1 for Tf, but no interaction of Hfe and Tfr1. Third, we used the transthyretin (TTR) promoter to specifically express an *Hfe* transgene in hepatocytes of mice lacking endogenous Hfe. The results obtained with all three strains support the conclusion that Hfe dissociated from Tfr1, and not the Hfe/Tfr1 complex, acts to induce hepcidin expression.

We suggest that Tfr1 normally acts to sequester Hfe and keep it inactive, and that competition between Fe-Tf and Hfe for Tfr1 binding is a key component of a liver-centered homeostatic regulatory mechanism. We speculate that Hfe released from Tfr1 interacts with Tfr2 to signal for hepcidin production.

## Results

### Generation of *Tfr1* mutant mice

To elucidate how the Hfe/Tfr1 interaction modulates iron homeostasis *in vivo*, we took advantage of mutagenesis studies done by Bjorkman and colleagues characterizing interactions between TFR1, HFE and TF (Giannetti and Bjorkman, 2004; Giannetti et al., 2003; West et al., 2001). The *in vitro* interaction profiles (Figure 1A) for the wild type and mutant murine proteins, as assessed by surface plasmon resonance (SPR) analysis, were comparable to those of their human counterparts. The R654A Tfr1 mutation completely abrogates diferric transferrin (Fe-Tf) binding and has no apparent effect on the interaction with Hfe. Furthermore, the L622A mutation, removing an amino acid critical for a van der Waals interaction between Hfe and Tfr1 but not for Tf binding, prevents Hfe-Tfr1 binding, but decreases the Tfr1 Fe-Tf interaction to a lesser extent (approximately 20-fold). The altered affinity for Tf should be inconsequential *in vivo*, where plasma Fe-Tf concentrations still far exceed the $K_d$ for binding. A model of action for wild type, R654A, and L622A Tfr1 is depicted in Figure 1B-D. We confirmed that the Fe uptake function of the mutant Tfr1 proteins was consistent with the *in vitro* binding data by stably expressing wild type, R654A or L622A Tfr1 in TRVb cells, which lack endogenous Tfr1 and Tfr2 (McGraw et al., 1987). When expressed at similar levels, L622A Tfr1 mediated uptake of $^{55}$Fe-Tf at a rate that was approximately half that of wild type Tfr1. In contrast, R654A Tfr1 had no apparent Fe-Tf uptake activity (Supplementary Fig. 1).

We previously observed that mice homozygous for a null *Tfr1* allele died of severe anemia during embryogenesis (Levy et al., 1999a), indicating that failure of the Tf cycle would have general effects that could confound our analysis. Mice with haploinsufficiency for *Tfr1* also have impaired erythropoiesis and slightly abnormal iron homeostasis (Levy et al., 1999a). For these reasons, we developed a mutant strain that expresses an R654A allele of *Tfr1* constitutively from a heterologous locus (ROSA26), leaving the endogenous Tfr1 locus intact (Supplementary Fig. 2A, B). We reasoned that the transgene product would not participate in the Tf cycle, but should form a complex with Hfe that would not be subject to competition from Tf.

We were able to use an alternative strategy to develop mice carrying the other Tfr1 mutation. Since L622A does not prevent Tf binding, we introduced a missense change resulting in that substitution directly into the endogenous murine *Tfr1* gene (Supplementary Fig. 2C, D). We will discuss analysis of these two mutant mouse strains individually.

### Analysis of mice expressing the *Tfr1* R654A transgene

Missense mutations in Tfr1 do not significantly alter its electrophoretic mobility. For this reason, we confirmed that animals expressing the *Tfr1* R654A transgene produced more Tfr1 protein by analyzing total liver extracts by western blot and comparing them to wild type and $Hfe^{-/-}$ mice (Figure 2A). *Tfr1* protein was increased in animals carrying the transgene. It was markedly decreased in livers from $Hfe^{-/-}$ mice, presumably because their high total body iron burden leads to destabilization of *Tfr1* mRNA through its iron regulatory elements (reviewed in (Eisenstein, 2000)). However, the mutant allele does not encode 3′ iron regulatory elements important for post-transcriptional regulation of the mRNA and, accordingly, Tfr1 was expressed at higher levels in $Hfe^{-/-}$ $ROSA26^{Tfr1R654A/+}$ mice carrying one copy of the transgene.

To confirm that expression of the *Tfr1* R654A transgene did not significantly impair the Tf cycle, we analyzed erythropoiesis by automated complete blood counts. As shown in Supplementary Table 1, all erythroid parameters were normal, indicating that *ROSA26*$^{Tfr1R654A/Tfr1R654A}$ mice had normal Tf cycle iron uptake in the erythron, the tissue that is most dependent upon that mechanism.

We next evaluated iron homeostasis in *ROSA26*$^{Tfr1R654A/Tfr1R654A}$ mice, comparing them with wild type and *Hfe*$^{-/-}$ mice. We reasoned that expression of R654A Tfr1, which is able to bind Hfe but not Tf, should promote a constitutive Hfe/Tfr1 interaction (Figure 1C). If Hfe requires Tfr1 to induce hepcidin expression, hepcidin mRNA should be increased in mice expressing the R654A Tfr1 transgene; therefore, the animals might show evidence of iron deficiency. On the other hand, if interaction with Tfr1 prevents Hfe from inducing hepcidin expression, the phenotype of *ROSA26*$^{Tfr1R654A/Tfr1R654A}$ mice should be similar to *Hfe*$^{-/-}$ mice, which lack Hfe altogether.

We found that *ROSA26*$^{Tfr1R654A/Tfr1R654A}$ mice had significantly increased occupancy of serum transferrin with iron (transferrin saturation), similar to *Hfe*$^{-/-}$ mice (Figure 2B). As was already shown in Supplementary Table 1, this was not due to decreased iron utilization for erythropoiesis. We can conclude, therefore, that more iron enters the serum. Increased transferrin saturation is a hallmark feature of clinical hemochromatosis. Mice carrying one allele of the R654A *Tfr1* transgene on an *Hfe*$^{-/-}$ background also had elevated transferrin saturation. The absolute amount of serum transferrin varied between animals and genotypes when evaluated by semi-quantitative immunoblotting and by measurement of total iron binding capacity (data not shown). Compared to wild type animals, it was not significantly different in *ROSA26*$^{Tfr1R654A/Tfr1R654A}$ or *Hfe*$^{-/-}$ *ROSA26*$^{Tfr1R654A/+}$ mice, but it was decreased in *Hfe*$^{-/-}$ mice. We do not yet have an explanation for this observation.

Liver non-heme iron content reflects the total body iron endowment, and it is increased in hemochromatosis. *ROSA26*$^{Tfr1R654A/Tfr1R654A}$ liver non-heme iron content was significantly increased as compared to wild type controls, but less than observed in *Hfe*$^{-/-}$ mice (Figure 2C). *Hfe*$^{-/-}$ *ROSA26*$^{Tfr1R654A/+}$ mice had liver non-heme iron content intermediate between *ROSA26*$^{Tfr1R654A/Tfr1R654A}$ and *Hfe*$^{-/-}$ animals. The histological pattern of iron deposition in *ROSA26*$^{Tfr1R654A/Tfr1R654A}$ mice was predominantly periportal, similar to that observed in *Hfe*$^{-/-}$ animals but to a lesser extent (Figure 2F-H).

Patients with advanced hemochromatosis can have increased non-heme iron deposition in the heart, which, if left untreated, can lead to cardiomyopathy. Analyzed at 10 weeks of age, our *Hfe*$^{-/-}$ mice were previously shown to have a modest increase in heart iron content (Miranda et al., 2003). Here, at 8 weeks, we found no significant difference in heart non-heme iron levels between wild type and *Hfe*$^{-/-}$ mice. Interestingly, however, *ROSA26*$^{Tfr1R654A/Tfr1R654A}$ mice did have significant heart iron loading (Figure 2D). We do not yet understand why *ROSA26*$^{Tfr1R654A/Tfr1R654A}$ mice accumulated more cardiac iron.

Increased TF saturation and tissue iron overload in *ROSA26*$^{Tfr1R654A/Tfr1R654A}$ mice suggest that an increased propensity for Hfe to interact with Tfr1 mimics the *Hfe*$^{-/-}$ phenotype. We predicted that, similar to *Hfe*$^{-/-}$ mice, the *ROSA26*$^{Tfr1R654A/Tfr1R654A}$ mice might express inappropriately low levels of hepcidin for their overall iron status. As shown in Figure 2E, iron overload in *ROSA26*$^{Tfr1R654A/Tfr1R654A}$ mice was accompanied by decreased hepcidin mRNA expression. The decrease in hepcidin expression in *ROSA26*$^{Tfr1R654A/Tfr1R654A}$ mice was not as severe as observed in *Hfe*$^{-/-}$ animals, perhaps because not all Hfe is constitutively bound to Tfr1. Nonetheless, taken together, our data reveal that mice constitutively expressing a mutant Tfr1 molecule that does not bind Tf but interacts normally with Hfe had a phenotype that was

similar, but not identical, to that of *Hfe*$^{-/-}$ mice. These data support the hypothesis that Hfe functions to induce hepcidin expression when it is not interacting with Tfr1.

## Analysis of mice carrying a L622A mutation within the endogenous *Tfr1* locus

To examine the role of the Hfe/Tfr1 complex from a different perspective, we introduced an L622A mutation into the endogenous *Tfr1* gene. This substitution should prevent interaction of Hfe with Tfr1 but should not significantly interfere with the Tf cycle *in vivo* (Figure 1D). We found that *Tfr1*$^{L622A/L622A}$ mice had a slight, yet significant, decrease in serum Tf saturation, though liver non-heme iron content was normal (Figure 3A, B). There was no evidence of excess iron deposition on examination of liver sections (data not shown). Complete blood counts revealed mild hypochromic, microcytic anemia in the L622A mutant animals, indicative of iron-deficient erythropoiesis (Table 1).

To determine whether decreased serum iron and iron-deficient erythropoiesis might be the consequences of increased hepcidin production, as previously observed in hepcidin transgenic mice (Nicolas et al., 2002; Roy et al., 2007), we examined liver hepcidin mRNA expression by quantitative PCR. In normal animals, hepcidin mRNA expression increases in response to iron loading (Pigeon et al., 2001). This response is blunted in *Hfe*$^{-/-}$ mice (Bridle et al., 2003b; Muckenthaler et al., 2003; Nicolas et al., 2003) and in *ROSA26*$^{Tfr1R654A/Tfr1R654A}$ mice (Figure 2E). In contrast, *Tfr1*$^{L622A/L622A}$ mice, which should have no interaction of Hfe with Tfr1, had an almost 2-fold increase in basal levels of liver hepcidin mRNA (Figure 3C). This increase in hepcidin likely explains the decreased Tf saturation and iron-deficient erythropoiesis in these animals.

## Analysis of *Hfe* transgenic mice

Thus far, our data were most consistent with the interpretation that Hfe signals to induce hepcidin expression when it is not in complex with Tfr1. Accumulating evidence suggests that Hfe acts in the hepatocyte itself, rather than in a different cell type. To further test both ideas, we developed *Hfe* transgenic mice by placing an *Hfe* cDNA under the control of the hepatocyte-specific transthyretin (TTR) promoter (Supplementary Figure 2E, F). This promoter mediates high level, hepatocyte-specific expression at all developmental stages in a copy number-independent fashion (Yan et al., 1990). Mice expressing the *Hfe* transgene were bred with *Hfe*$^{-/-}$ mice of the same genetic background to produce animals lacking expression of endogenous *Hfe*, with high levels of transgenic *Hfe* mRNA produced only in the liver (Supplementary Figure 3).

We compared mice carrying the transgene on an *Hfe*$^{-/-}$ background to both *Hfe*$^{-/-}$ and wild type animals. We found that the transgene not only corrected the increased Tf saturation and liver iron overload in *Hfe*$^{-/-}$ mice, but also caused iron deficiency (Figure 4A, B). *Hfe*$^{-/-}$ mice carrying the transgene had lower Tf saturation and less hepatic non-heme iron than wild type controls. Furthermore, while *Hfe*$^{-/-}$ animals displayed greatly increased liver iron loading in periportal regions of the liver as expected, *Hfe*$^{-/-}$ animals expressing the transgene had less stainable hepatic iron than wild type animals (Figure 4D-F). Accordingly, complete blood counts revealed that the transgenic *Hfe*$^{-/-}$ animals had a hypochromic, microcytic anemia attributable to severe iron deficiency (Table 2). Analysis of liver tissue revealed that *Hfe*$^{-/-}$ mice carrying the transgene not only expressed more hepcidin mRNA than *Hfe*$^{-/-}$ mice, but also expressed more hepcidin than wild type controls (Figure 4C). Elevated hepcidin expression, inappropriate for body iron stores, likely accounts for their iron deficient and anemic phenotype. Because Hfe is expressed at high levels in the transgenic mice, these results further support the conclusion that hepatocyte Hfe, unbound to Tfr1, signals to induce hepcidin expression.

Recently, Enns and colleagues reported that both HFE and iron-loaded TF stabilize TFR2 protein in human hepatoma cells (Chen et al., 2007; Johnson et al., 2007). We observed that the amount of hepatic Tfr2 protein is increased in *Hfe*$^{-/-}$ animals but markedly decreased after expression of the Hfe transgene in *Hfe*$^{-/-}$ mice (Figure 4G). These observations are consistent with the interpretation that Tfr2 is stabilized by increased Tf saturation in *Hfe*$^{-/-}$ mice, and that the stabilization does not occur when Tf saturation is lowered by expression of the Hfe transgene. Thus, while Hfe may play some role in the stabilization of Tfr2, under these circumstances Tf saturation appears to be the dominant factor.

## Discussion

Most patients with hemochromatosis are homozygous for a missense mutation altering the gene encoding HFE. HFE forms a protein-protein complex with TFR1, a protein important for cellular iron uptake. Although these facts have been known for more than a decade, the molecular function of HFE is not yet understood. Recent studies indicate that HFE is involved in modulating the expression of hepcidin, but how it does so is not known. We set out to explore the role of the murine Hfe/Tfr1 complex *in vivo* by deliberately altering the stoichiometry of its component proteins. We developed one mouse model in which Hfe should constitutively interact with Tfr1, and two other models in which most or all Hfe should be free of Tfr1. Our results suggest that Tfr1 serves to sequester Hfe, and that Hfe acts to induce hepcidin expression when it is independent of Tfr1 in hepatocytes.

We had unintentionally examined the effects of changing the stoichiometry of the Hfe/Tfr1 interaction in earlier experiments studying *Tfr1*$^{+/-}$ mice (Levy et al., 1999a; Levy et al., 2000). We observed that animals lacking one endogenous *Tfr1* allele had decreased hepatic iron stores and evidence of iron-restricted erythropoiesis. While there are several possible reasons for this observation, it could be explained by an increase in Hfe that is not associated with Tfr1, and a consequent increase in hepcidin production. Accordingly, we later showed that *Tfr1*$^{+/-}$ mice produce increased hepcidin mRNA (C.N. Roy and N.C.A., unpublished observations). A model in which Tfr1 normally sequesters Hfe reconciles these findings. We suggest that haploinsufficiency for *Tfr1* results in more unbound Hfe, signaling for an increase of hepcidin expression.

Although the mutant mouse strains described in this report have been instructive, there are several observations that we do not fully understand. First, mice expressing the R654A Tfr1 transgene do not accumulate as much iron as *Hfe*$^{-/-}$ mice. This may be because there is still some Hfe that is not interacting with the mutant Tfr1. Additionally, it is possible that the mutant Tfr1 protein forms heterodimers with wild type Tfr1, impairing normal Tf uptake. If this occurs, however, our data indicate it is clearly not an issue in the erythron, where we previously showed the Tf cycle to be most important (Levy et al., 1999a).

We also observed that animals carrying the R564A transgene on an *Hfe*$^{-/-}$ background have a milder phenotype than *Hfe*$^{-/-}$ mice, even though there is no Hfe produced. Along the same lines, we previously observed that *Hfe*$^{-/-}$ mice lacking one *Tfr1* allele (*Hfe*$^{-/-}$ *Tfr*$^{+/-}$) had more iron overload than *Hfe*$^{-/-}$ mice with both *Tfr* alleles intact (Levy et al., 2000). These results suggest that Tfr1 may interact with another protein important for regulation of iron homeostasis. It is conceivable that mutations in Tfr1 have some impact on the function of Tfr2, even though they do not appear to heterodimerize to any great extent (Vogt et al., 2003). Alternatively, there may be another protein that is structurally similar to Hfe, which interacts with Tfr1 in a comparable fashion. Accordingly, there is some evidence that classical major histocompatibility class I molecules may be involved in iron homeostasis (Cardoso et al., 2002).

Atransferrinemia is a distinct iron overload disorder, resulting from mutations in the gene encoding in serum TF (Beutler et al., 2000; Trenor et al., 2000). Affected patients and mice suffer severe microcytic anemia due to iron-restricted erythropoiesis, but manifest iron overload in non-hematopoietic tissues. We propose that Tfr1 normally acts to sequester Hfe, and that increasing $Fe_2$-Tf causes a competition with Hfe for Tfr1 binding. In $Tf^{hpx/hpx}$ mice, a lack of Tf prevents this competition. As a result, a disproportionately large amount of Hfe may remain constitutively bound to Tfr1 and be unable to signal for the upregulation of hepcidin. Our hypothesis correctly predicts that $Tf^{hpx/hpx}$ animals should hyperaccumulate iron even though they are severely anemic. This situation is similar to the mouse model expressing the R564A *Tfr1* transgene from the ROSA locus, which should form the Hfe-Tfr1 complex constitutively.

Mutations in both *HFE* and *TFR2* are known to cause hemochromatosis. Hfe and Tfr2 interact in cultured cells, and Tfr2 competes with Tfr1 for Hfe binding (Goswami and Andrews, 2006). It is reasonable to expect that, under normal homeostatic conditions, Hfe is partitioned between Tfr1, Tfr2 and possibly other proteins. As Tf saturation increases, Tf likely displaces Hfe from Tfr1. Furthermore, increased Tf saturation results in stabilization of Tfr2 protein (Johnson and Enns, 2004; Robb and Wessling-Resnick, 2004), and degradation of Tfr1 mRNA (Eisenstein, 2000). All of these effects should shift Hfe away from interaction with Tfr1 and towards interaction with Tfr2, as depicted in our working model (Figure 5). Conversely, low iron conditions should favor interaction between Hfe and Tfr1. As we show in our Tfr1 mutant mouse models, as Hfe is uncoupled from Tfr1 binding, hepcidin levels are upregulated. We propose that an Hfe/Tfr2 complex helps to propagate a signaling cascade resulting in the upregulation of hepcidin and, consequently, decreased dietary iron uptake and decreased macrophage iron release. Mutations in either *HFE* or *TFR2* would impair this putative signaling complex, causing a failure to properly upregulate hepcidin, resulting in clinical hemochromatosis.

## Experimental Procedures

### SPR analysis of mutant Tfr1

The soluble mouse Tfr1 ectodomain was cloned and produced analogously to the human TFR1 previously described (Lebron et al., 1999; West et al., 2001). After subcloning Tfr1 into the pACGP67A baculovirus expression vector, L622A and R654A mutations were introduced using the QuikChange mutagenesis kit (Stratagene). Baculovirus supernatants containing the secreted receptor were used in a surface plasmon resonance (SPR) assay as previously described (Giannetti and Bjorkman, 2004; Giannetti et al., 2003). Mouse Hfe was produced as previously described (Lebron et al., 1999) by co-expression of the mouse Hfe heavy chain with human β2-microglobulin in CHO cells. Protein was purified from concentrated CHO-cell supernatants using a BBM.1 (anti human-β2-microglobulin) column and eluted with 50 mM diethylamine pH 11.5 into tubes containing 1 M Tris pH 7.4 to preserve purity. Eluted protein was further purified on an S-200 sizing column to eliminate small quantities of aggregate. Apo-mouse transferrin was purchased from Sigma, loaded with iron as previously described (Giannetti et al., 2003) and purified on an S-200 sizing column. All biosensor experiments were performed as previously described (Giannetti and Bjorkman, 2004; Giannetti et al., 2003) with the exception that data reduction, double referencing, and analysis was performed with the Scrubber II software package (BioLogic Software). A simple 1:1 binding model could describe the binding interactions with the mouse proteins, rather than the more complex bivalent ligand model used for the human system.

### Oligonucleotide primers

Oligonucleotide primers are listed in Supplementary Table 2.

### Iron uptake by mutant Tfr1 molecules

We mutated the vector pBS$^+$ Tfr1, containing the complete mouse *Tfr1* cDNA, using the QuikChange site-directed mutagenesis kit (Stratagene) and primers PS-9 and PS-10 to create the L622A mutation. Primers PS-11 and PS-12 were used to create the R654A mutation. The wild type, L622A, and R654A *Tfr1* cDNA-containing vectors were amplified with primers PS-48 and PS-49 to insert a BamHI site immediately before the translational start codon, and an XhoI site in place of the endogenous stop codon. These PCR products were purified with the Qiagen PCR purification kit, digested with BamHI and XhoI, and ligated into pcDNA3.1 V5/His (Invitrogen). Sequence analysis demonstrated that the Myc epitope tag in each vector was out of frame. In order to place the epitope tag of each expression vector into frame, all three constructs were mutagenized with the QuikChange kit using the primers PS-62 and PS-63. Final sequence analysis showed that the vectors contained the correct sequence. The vectors containing WT, L622A, and R654A forms of the Tfr1 cDNA were named pPJS040, -041, and -042, respectively. Stable clones were obtained in TRVb cells, which contain no endogenous Tfr1 (McGraw et al., 1987), by electroporation and then selection with 400 μg/ml G418 (Invitrogen). Cells were grown in HamF12 media supplemented with 5% fetal bovine serum, 1% penicillin/streptomycin, 1% L-glutamine, and 2g/L dextrose, and maintained under selection in 400 μg/ml G418.

$^{55}$Fe-Tf preparation and uptake procedures were modified from a previously described protocol (Roy et al., 1999). $^{55}FeCl_3$ (Amersham Biosciences) was complexed to nitrilotriacetic acid (NTA) by adding $^{55}FeCl_3$ to 1 ml 0.1 M NTA solution (1:50 ratio Fe:NTA). Then, four-fold excess $^{55}$Fe-NTA was incubated with murine apo-Tf for 1.5 hours in carbonate buffer (10 mM $NaHCO_3$, 0.25 M Tris-HCl). $^{55}$Fe-Tf was separated from free $^{55}$Fe on a 3-ml G-50 Sephadex (Sigma) column. The resulting Tf was nearly completely saturated with iron.

To determine the rate of Tf-Fe uptake into the stable Tfr1-TRVb cell lines, cells were plated below confluence in 6-well dishes. Plates were washed two times with serum free media (HamF12, 20 mM Hepes) and preincubated at 37°C, and 5% $CO_2$ for 15 minutes. Plates were removed and the medium aspirated. 1.0 ml of specific medium (100 nM $^{55}$Fe-Tf, 2 mg/ml ovalbumin) was added to 4 wells for each time point (0, 45, 90, 135, and 225 minutes). Non-specific ligand (same as specific medium with the addition of 10-fold excess cold Tf-Fe) was added to two wells for each time point, and all were placed at 37°C 5% $CO_2$. Cells were placed on ice at a given time point and the medium was aspirated. Externally bound Tf was stripped by incubation with 2.0 ml of acidic buffer (0.5 N acetic acid, 0.5 M NaCl, 1 mM $FeCl_3$) for 3 minutes. Cells were washed three times with final wash solution (150 mM NaCl, 20 mM HEPES pH 7.4, 1 mM $CaCl_2$, 5 mM KCl, 1 mM $MgCl_2$) on ice. Cells were solubilized in 1.0 ml 0.1% Triton X-100, 0.1 N NaOH and counted in a gamma counter.

### Generation of *ROSA26$^{Tfr1R654A/Tfr1R654A}$* mice

To generate the transgenic ROSA26 R654A *Tfr1* targeting vector, mouse *Tfr1* cDNA contained within plasmid pBS$^+$-TFR1 was mutagenized with the QuikChange kit as described earlier. The insert was liberated with SacI and NotI, gel-purified, and ligated into plasmid pBigT (kind gift of Frank Costantini). The resultant plasmid was digested with PacI and AscI and recessed 3′ ends were filled with DNA Polymerase I large (Klenow) fragment (New England Biolabs). This fragment was ligated into a similarly filled XbaI site in pROSA26-1 (kind gift of Philippe Soriano). The final vector was analyzed by DNA sequencing and named pPJS022. This plasmid was linearized with KpnI and gel-purified away from vector sequence using the Geneclean kit (Bio101) and electroporated into J1 embryonic stem cells (129 background). Cells were selected for resistance to G418 and ganciclovir. Correctly targeted clones were identified by both Southern blotting and PCR analysis, and were karyotyped to confirm a correct complement of mouse chromosomes. The Mental Retardation Research Center Gene

Manipulation Facility at Children's Hospital Boston carried out blastocyst injections. Founders were identified by southern blot analysis and/or PCR genotyping of tail DNA, and residual vector sequences were removed *in vivo* by breeding to E2A-Cre transgenic mice.

### Generation of *Tfr1*$^{L622A/L622A}$ mice

To generate the L622A knock-in *Tfr1* allele, two 4kb arms of the murine *Tfr1* gene were amplified from a mouse 129Sv/J bacterial artificial chromosome library using primers PS-1 and PS-2 for the 5′ fragment, and PS-3 and PS-24 for the 3′ fragment. Each PCR product was subcloned into the pCR2.1-TOPO (Clontech) cloning vector. The L622A mutation was inserted into exon 17 of the 5′ fragment with the QuikChange site-directed mutagenesis kit using primers described earlier. The 5′-fragment containing vector was digested with ClaI, 3′ overhangs were filled with Klenow enzyme, and the product then further digested with XhoI. This fragment was gel-purified with the Gene Clean Spin kit, and then subcloned into vector pNTKBLP between the HpaI and XhoI sites. pNTKBLP is the pKO Scrambler NTKV-1907 (Stratagene) backbone with the neomycin cassette excised with AscI. A floxed neomycin cassette was released from its vector backbone with NotI, overhangs were filled with Klenow enzyme, and the resulting fragment was cloned into pKO Scrambler NTKV-1907 to produce pNTKBLP. The 3′ arm of the *Tfr1* sequence was liberated with a SacII and XmaI digestion, gel-purified, and ligated into the pNTKBLP vector already containing the 5′ region. The final vector (pPJS015) was sequenced to confirm the correct DNA sequence of each exon and exon/intron boundary. This construct was introduced into J1 ES cells by electroporation after linearization with PvuI, and cells were selected for resistance to both G418 and ganciclovir. Correctly targeted mutants were identified by Southern blot analysis. The targeting efficiency was approximately 7%. Five positive clones were karyotyped, and two were selected for injection. ES cells containing the correctly targeted *Tfr1* allele injected into C57BL/6J blastocysts at the Children's Hospital Boston Center for Molecular developmental hematopoiesis. Founders were identified by southern blot and/or PCR analysis. The neomycin selection cassette was removed by Cre-loxP recombination after breeding to E2A-Cre transgenic mice. All mice homozygous for the L622A mutated allele were generated from a cross of *Tfr1*$^{L622A/L622A}$ parents.

### Generation of transgenic mice expressing Hfe under control of the *transthyretin* (*TTR*) promoter

The complete 1.1kb mouse *Hfe* cDNA was amplified using the primers HFEtgREV and HFEtgFOR from a cDNA template contained in pcDNA3.1, and subcloned into pCR2.1-TOPO. This fragment was liberated with SpeI and EcoRV. The 3′ overhangs were filled with Klenow enzyme, and the resulting sequence ligated into the blunted StuI site in the pTTR1exV3 vector (kind gift of Terry Van Dyke). Correct orientation and sequence were confirmed by sequencing analysis. The excised HindIII fragment was purified from the vector by electroelution and microinjected into C57BL/6 oocyte pronuclei at the Children's Hospital Boston Center for Molecular Developmental Hematopoiesis. These mice were bred with an *Hfe*$^{-/-}$ strain of the same genetic background to generate *Hfe*$^{-/-}$ animals carrying the integrated TTR-Hfe transgene.

### Animal care and analysis

All mice were born and housed in the barrier facility at the Children's Hospital Boston according to approved protocols. Animals were maintained on the Prolab RMH 300 diet (PMI nutrition). The facility employs a constant dark-night light cycle, and all animals were provided both water and food *ad libitum*. Due to inherent differences in iron metabolism between male and female animals, only females were employed for analysis. All animals were euthanized at 8-weeks of age for analysis.

### Southern blot and PCR genotyping

The Puregene DNA isolation kit (Gentra Systems) was used to prepare genomic DNA from tail snips. For Southern blot analysis, DNA (10 μg) was digested overnight and fractionated on a 0.7% agarose gel and then transferred to Hybond $N^+$ membrane (Amersham). Blots were probed with a $^{32}$P-dCTP-labeled product. Genomic DNA from mice containing the L622A mutation was digested with BamHI, and probed with a labeled PCR product amplified using primers PS-36 and PS-37 to genotype the 5′ end of the insertion. The 3′ end of the gene was probed with a labeled PCR product amplified using primers PS-38 and PS-39. These mice were also PCR genotyped using the forward primer PS-71a and reverse primer L622AF giving either a 292bp band for the targeted allele or a 269bp for the WT allele. Genomic DNA from ROSA26-R654A mice was digested with EcoRV and probed a PCR product amplified with primers ROSA A and ROSA B. Mice were also PCR genotyped using primers PS-64a and PS-65. The same forward primer and the reverse primer PS-102 produces a 614 bp band for the mutant allele. Transgenic TTR-HFE mice were PCR genotyped with primers PS-133 and PS-134 yielding a 450bp band.

### Tissue iron staining

Tissue samples of liver and spleen were fixed in 10% buffered formalin for 24 hours and then embedded in paraffin. Deparaffinized sections of tissue were stained with DAB-enhanced Perls iron stain by the Children's Hospital Boston Pathology Laboratory.

### Blood and tissue iron analysis

Whole blood for complete blood counts was collected retro-orbitally into EDTA-coated microtainer tubes (Becton Dickinson) from animals anesthetized with Avertin (Sigma). Samples were analyzed on an Avida 120 analyzer (Bayer) by the Clinical Core Laboratories located at Children's Hospital Boston. Whole blood was collected by retro-orbital bleeding in serum separator tubes (Becton Dickinson), and serum was prepared according to the manufacturer's instructions. Serum iron values were determined with the Serum Iron/UIBC kit (ThermoDMA) according to manufacturer instructions. Liver and spleen tissues were collected and tissue non-heme iron concentrations were determined as previously described (Levy et al., 1999a; Torrance and Bothwell, 1980).

### RNA extraction, RT-PCR and quantitative PCR

Total liver RNA was isolated from flash-frozen tissue employing RNA STAT-60 (Leedo Medical Laboratories). Total RNA was treated with DNase I (Roche) to remove contaminating genomic DNA as per manufacturers' instructions. cDNA was synthesized from the resulting RNA using the iScript cDNA Synthesis Kit (Bio-Rad) according to manufacturers' protocol. Real-time quantification of hepcidin and β-actin mRNA transcript levels was done with the iQ SYBR Green Supermix (Bio-Rad) in a 20 μl reaction in the iCycler (Bio-Rad) instrument according to manufacturers' instructions. Hepcidin mRNA was amplified using primers Hamp1 F and Hamp1 R. Control β-actin mRNA was amplified using primers β-actin F and β-actin R as previously described (Nemeth et al., 2004a). Amplification conditions were as follows: 95°C for 3 minutes and then 95°C for 10 sec, 60°C for 45 sec for 45 cycles. Transcript abundance of hepcidin was calculated in triplicate relative to the expression of the stable housekeeping gene β-actin, and then presented as a ratio to the wild type control in each experiment. The average relative expression of hepcidin in wild type 129SvEv/Tac animals was assigned an arbitrary value of 1 in each experiment.

### Immunoblot analysis

Liver tissue was manually lysed in modified RIPA buffer (50 mM Tris pH 7.5, 150 mM NaCl, 1% NP-40, 0.5% sodium deoxycholate, 0.1% SDS). Cultured cells were washed with cold

PBS, scraped into PBS, pelleted gently, and lysed in IP lysis buffer (150 mM NaCl, 50 mM Tris-HCl pH 8.0, 1% Triton X-100). Cell debris was removed by centrifugation. 75 or 150 μg of total tissue protein, or 40 μg cell lysate was diluted in 2X Laemmli buffer (0.2 M DTT final), boiled and subjected to electrophoresis through 8% or 10% polyacrylamide gels. The proteins were transferred onto nitrocellulose membranes and immunoblot analysis was performed using mouse anti-hTFR1 (1:1000, Zymed), rabbit anti-mouse Tfr2 (1:1000, Alpha Diagnostic International) or rabbit anti-β-actin (1:1000, Cell Signaling). Blots were then incubated with either anti-mouse or anti-rabbit secondary antibody conjugated to horseradish peroxidase (1:5000) and then subjected to chemiluminescence (Amersham, ECL) per the manufacturer's directions.

## Supplementary Material

Refer to Web version on PubMed Central for supplementary material.

### Acknowledgements

This work was supported by NIH R01 DK53813 (N.C.A.) and NIH K01 DK074410 (P.J.S.). We would also like to thank the following investigators for reagents: Frank Costantini for the pBigT vector, Philippe Soriano for the pROSA26-1 vector, and Terry Van Dyke for the pTTR1exV3 vector. We thank Margaret Thompson and the Children's Hospital Boston Mental Retardation Research Center Gene Manipulation Facility (NIH P30 HD018655) for blastocyst injections, and Yuko Fujiwara and the Children's Hospital Boston Center for Molecular Developmental Hematopoiesis for blastocyst injections and pronuclei microinjections (NIH P30 DK49216-14). Finally, we thank Adriana Donovan and Cindy Roy for technical advice and helpful suggestions, Kristina Roberts and Tom Bartnikas for reviewing the manuscript, and members of the Andrews and Fleming labs for helpful discussions. The authors have no competing financial interests. A.M.G. and P.J.B. designed the Tfr1 mutations and analyzed the protein interactions *in vitro*. P.J.S. and N.C.A. conceived and designed the murine experiments, analyzed the data and wrote the manuscript. P.T.T. maintained the mouse colony and assisted in phenotyping the animals.

## References

Aisen P, Listowsky I. Iron transport and storage proteins. Annual Reviews of Biochemistry 1980;49:357–393.

Ajioka RS, Levy JE, Andrews NC, Kushner JP. Regulation of iron absorption in Hfe mutant mice. Blood 2002;100:1465–1469. [PubMed: 12149232]

Bennett MJ, Lebron JA, Bjorkman PJ. Crystal structure of the hereditary haemochromatosis protein HFE complexed with transferrin receptor. Nature 2000;403:46–53. [PubMed: 10638746]

Beutler E, Gelbart T, Lee P, Trevino R, Fernandez MA, Fairbanks VF. Molecular characterization of a case of atransferrinemia. Blood 2000;96:4071–4074. [PubMed: 11110675]

Bralet MP, Duclos-Vallee JC, Castaing D, Samuel D, Guettier C. No hepatic iron overload 12 years after liver transplantation for hereditary hemochromatosis. Hepatology 2004;40:762. [PubMed: 15349921] author reply 762

Bridle KR, Frazer DM, Wilkins SJ, Dixon JL, Purdie DM, Crawford DH, Subramaniam VN, Powell LW, Anderson GJ, Ram GA. Disrupted hepcidin regulation in HFE-associated haemochromatosis and the liver as a regulator of body iron homoeostasis. Lancet 2003a;361:669–673. [PubMed: 12606179]

Bridle KR, Frazer DM, Wilkins SJ, Dixon JL, Purdie DM, Crawford DH, Subramaniam VN, Powell LW, Anderson GJ, Ramm GA. Disrupted hepcidin regulation in HFE-associated haemochromatosis and the liver as a regulator of body iron homoeostasis. Lancet 2003b;361:669–673. [PubMed: 12606179]

Cardoso EM, Macedo MG, Rohrlich P, Ribeiro E, Silva MT, Lemonnier FA, de Sousa M. Increased hepatic iron in mice lacking classical MHC class I molecules. Blood 2002;100:4239–4241. [PubMed: 12393413]

Cavill I, Worwood M, Jacobs A. Internal regulation of iron absorption. Nature 1975;256:328–329. [PubMed: 1143336]

Chen J, Chloupkova M, Gao J, Chapman-Arvedson TL, Enns CA. HFE modulates transferrin receptor 2 levels in hepatoma cells via interactions that differ from transferrin receptor 1/ HFE interactions. J Biol Chem. 2007pre-published online

Donovan A, Lima CA, Pinkus JL, Pinkus GS, Zon LI, Robine S, Andrews NC. The iron exporter ferroportin/Slc40a1 is essential for iron homeostasis. Cell Metab 2005;1:191–200. [PubMed: 16054062]

Eisenstein RS. Iron regulatory proteins and the molecular control of mammalian iron metabolism. Ann Rev Nutr 2000;20:627–662. [PubMed: 10940348]

Feder JN, Penny DM, Irrinki A, Lee VK, Lebron JA, Watson N, Tsuchihashi Z, Sigal E, Bjorkman PJ, Schatzman RC. The hemochromatosis gene product complexes with the transferrin receptor and lowers its affinity for ligand binding. Proc Natl Acad Sci U S A 1998;95:1472–1477. [PubMed: 9465039]

Giannetti AM, Bjorkman PJ. HFE and transferrin directly compete for transferrin receptor in solution and at the cell surface. J Biol Chem 2004;279:25866–25875. [PubMed: 15056661]

Giannetti AM, Snow PM, Zak O, Bjorkman PJ. Mechanism for multiple ligand recognition by the human transferrin receptor. PLoS biology 2003;1:E51. [PubMed: 14691533]

Goswami T, Andrews NC. Hereditary hemochromatosis protein, HFE, interaction with transferrin receptor 2 suggests a molecular mechanism for mammalian iron sensing. J Biol Chem 2006;281:28494–28498. [PubMed: 16893896]

Johnson MB, Chen J, Murchison N, Green FA, Enns CA. Transferrin receptor 2: evidence for ligand-induced stabilization and redirection to a recycling pathway. Mol Biol Cell 2007;18:743–754. [PubMed: 17182845]

Johnson MB, Enns CA. Regulation of transferrin receptor 2 by transferrin: diferric transferrin regulates transferrin receptor 2 protein stability. Blood 2004;104:4287–93. [PubMed: 15319290]

Lebron JA, Bennett MJ, Vaughn DE, Chirino AJ, Snow PM, Mintier GA, Feder JN, Bjorkman PJ. Crystal structure of the hemochromatosis protein HFE and characterization of its interaction with transferrin receptor. Cell 1998;93:111–123. [PubMed: 9546397]

Lebron JA, Bjorkman PJ. The transferrin receptor binding site on HFE, the class I MHC-related protein mutated in hereditary hemochromatosis. J Mol Biol 1999;289:1109–1118. [PubMed: 10369785]

Lebron JA, West AP Jr. Bjorkman PJ. The hemochromatosis protein HFE competes with transferrin for binding to the transferrin receptor. J Mol Biol 1999;294:239–245. [PubMed: 10556042]

Levy JE, Jin O, Fujiwara Y, Kuo F, Andrews NC. Transferrin receptor is necessary for development of erythrocytes and the nervous system. Nat Genet 1999a;21:396–399. [PubMed: 10192390]

Levy JE, Montross LK, Andrews NC. Genes that modify the hemochromatosis phenotype in mice. J Clin Invest 2000;105:1209–1216. [PubMed: 10791995]

Levy JE, Montross LK, Cohen DE, Fleming MD, Andrews NC. The C282Y mutation causing hereditary hemochromatosis does not produce a null allele. Blood 1999b;94:9–11. [PubMed: 10381492]

McGraw TE, Greenfield L, Maxfield FR. Functional expression of the human transferrin receptor cDNA in Chinese hamster ovary cells deficient in endogenous transferrin receptor. J Cell Biol 1987;105:207–214. [PubMed: 3611186]

Miranda CJ, Makui H, Soares RJ, Bilodeau M, Mui J, Vali H, Bertrand R, Andrews NC, Santos MM. Hfe deficiency increases susceptibility to cardiotoxicity and exacerbates changes in iron metabolism induced by doxorubicin. Blood 2003;102:2574–2580. [PubMed: 12805055]

Muckenthaler M, Roy CN, Custodio AO, Minana B, deGraaf J, Montross LK, Andrews NC, Hentze MW. Regulatory defects in liver and intestine implicate abnormal hepcidin and Cybrd1 expression in mouse hemochromatosis. Nat Genet 2003;34:102–107. [PubMed: 12704390]

Nemeth E, Rivera S, Gabayan V, Keller C, Taudorf S, Pedersen BK, Ganz T. IL-6 mediates hypoferremia of inflammation by inducing the synthesis of the iron regulatory hormone hepcidin. J Clin Invest 2004a;113:1271–1276. [PubMed: 15124018]

Nemeth E, Tuttle MS, Powelson J, Vaughn MB, Donovan A, Ward DM, Ganz T, Kaplan J. Hepcidin regulates cellular iron efflux by binding to ferroportin and inducing its internalization. Science 2004b; 306:2090–2093. [PubMed: 15514116]

Nicolas G, Bennoun M, Porteu A, Mativet S, Beaumont C, Grandchamp B, Sirito M, Sawadogo M, Kahn A, Vaulont S. Severe iron deficiency anemia in transgenic mice expressing liver hepcidin. Proc Natl Acad Sci U S A 2002;99:4596–4601. [PubMed: 11930010]

Nicolas G, Viatte L, Lou DQ, Bennoun M, Beaumont C, Kahn A, Andrews NC, Vaulont S. Constitutive hepcidin expression prevents iron overload in a mouse model of hemochromatosis. Nat Genet 2003;34:97–101. [PubMed: 12704388]

Parkkila S, Waheed A, Britton RS, Bacon BR, Zhou XY, Tomatsu S, Fleming RE, Sly WS. Association of the transferrin receptor in human placenta with HFE, the protein defective in hereditary hemochromatosis. Proc Natl Acad Sci U S A 1997;94:13198–13202. [PubMed: 9371823]

Pigeon C, Ilyin G, Courselaud B, Leroyer P, Turlin B, Brissot P, Loreal O. A new mouse liver-specific gene, encoding a protein homologous to human antimicrobial peptide hepcidin, is overexpressed during iron overload. J Biol Chem 2001;276:7811–7819. [PubMed: 11113132]

Robb A, Wessling-Resnick M. Regulation of transferrin receptor 2 protein levels by transferrin. Blood 2004;104:4294–4299. [PubMed: 15319276]

Roy CN, Mak HH, Akpan I, Losyev G, Zurakowski D, Andrews NC. Hepcidin antimicrobial peptide transgenic mice exhibit features of the anemia of inflammation. Blood 2007;109:4038–4044. [PubMed: 17218383]

Roy CN, Penny DM, Feder JN, Enns CA. The hereditary hemochromatosis protein, HFE, specifically regulates transferrin-mediated iron uptake in HeLa cells. J Biol Chem 1999;274:9022–9028. [PubMed: 10085150]

Spasic MV, Kiss J, Herrmann T, Kessler R, Stolte J, Galy B, Rathkolb B, Wolf E, Stremmel W, Hentze MW, et al. Physiologic systemic iron metabolism in mice deficient for duodenal Hfe. Blood 2007;109:4511–4517. [PubMed: 17264297]

Taylor MR, Gatenby PB. Iron absorption in relation to transferrin saturation and other factors. Br J Haematol 1966;12:747–753. [PubMed: 5925456]

Torrance, JD.; Bothwell, TH. Tissue iron stores. 1. Churchill Livingstone; New York: 1980.

Trenor CC 3rd, Campagna DR, Sellers VM, Andrews NC, Fleming MD. The molecular defect in hypotransferrinemic mice. Blood 2000;96:1113–1118. [PubMed: 10910930]

Vogt TM, Blackwell AD, Giannetti AM, Bjorkman PJ, Enns CA. Heterotypic interactions between transferrin receptor and transferrin receptor 2. Blood 2003;101:2008–2014. [PubMed: 12406888]

Waheed A, Parkkila S, Saarnio J, Fleming RE, Zhou XY, Tomatsu S, Britton RS, Bacon BR, Sly WS. Association of HFE protein with transferrin receptor in crypt enterocytes of human duodenum. Proc Natl Acad Sci U S A 1999;96:1579–1584. [PubMed: 9990067]

Weinstein DA, Roy CN, Fleming MD, Loda MF, Wolfsdorf JI, Andrews NC. Inappropriate expression of hepcidin is associated with iron refractory anemia: implications for the anemia of chronic disease. Blood 2002;100:3776–3781. [PubMed: 12393428]

West AP Jr. Giannetti AM, Herr AB, Bennett MJ, Nangiana JS, Pierce JR, Weiner LP, Snow PM, Bjorkman PJ. Mutational analysis of the transferrin receptor reveals overlapping HFE and transferrin binding sites. J Mol Biol 2001;313:385–397. [PubMed: 11800564]

Yan C, Costa RH, Darnell JE Jr. Chen JD, Van Dyke TA. Distinct positive and negative elements control the limited hepatocyte and choroid plexus expression of transthyretin in transgenic mice. EMBO J 1990;9:869–878. [PubMed: 1690125]

Zhang AS, Xiong S, Tsukamoto H, Enns CA. Localization of iron metabolism-related mRNAs in rat liver indicate that HFE is expressed predominantly in hepatocytes. Blood 2004;103:1509–1514. [PubMed: 14563638]

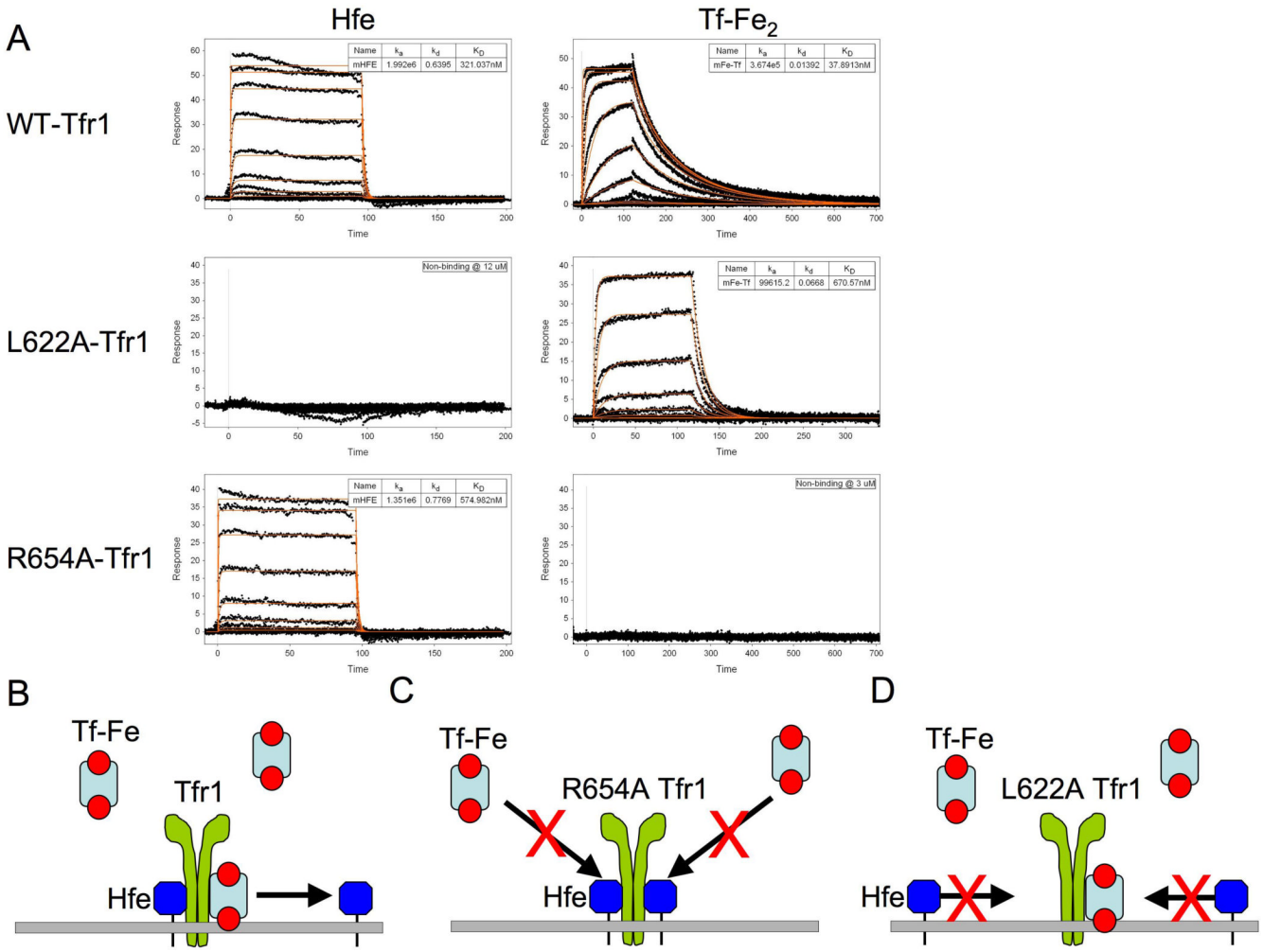


**Figure 1. SPR analysis of murine Hfe and diferric transferrin binding to mutant and wild type Tfr1**

Experimentally observed responses (A) are shown as black dots with best fit binding curves (red lines) derived from a 1:1 interaction model superimposed. The highest concentration protein injections are 12 μM (Hfe) and 3 μM (Fe-Tf) with subsequent injections related by a 3-fold dilution series. No binding was observed at these concentrations for Hfe binding to L622A-Tfr1 or Fe-Tf binding R654A-Tfr1. Given the concentration of proteins and the sensitivity of the SPR experiment, this suggests that the binding constants are weaker than 300 μM for Hfe and 30 μM for Fe-Tf. This is well above the physiological concentration of transferrin in serum. Model of action for wild type (B), R654A (C) and L622A (D) Tfr1 mutant proteins. The R654A Tfr1 mutation prevents Tf, but not Hfe, interaction with Tfr1. The L622A Tfr1 mutation prevents Hfe, but not Tf, binding to Tfr1.

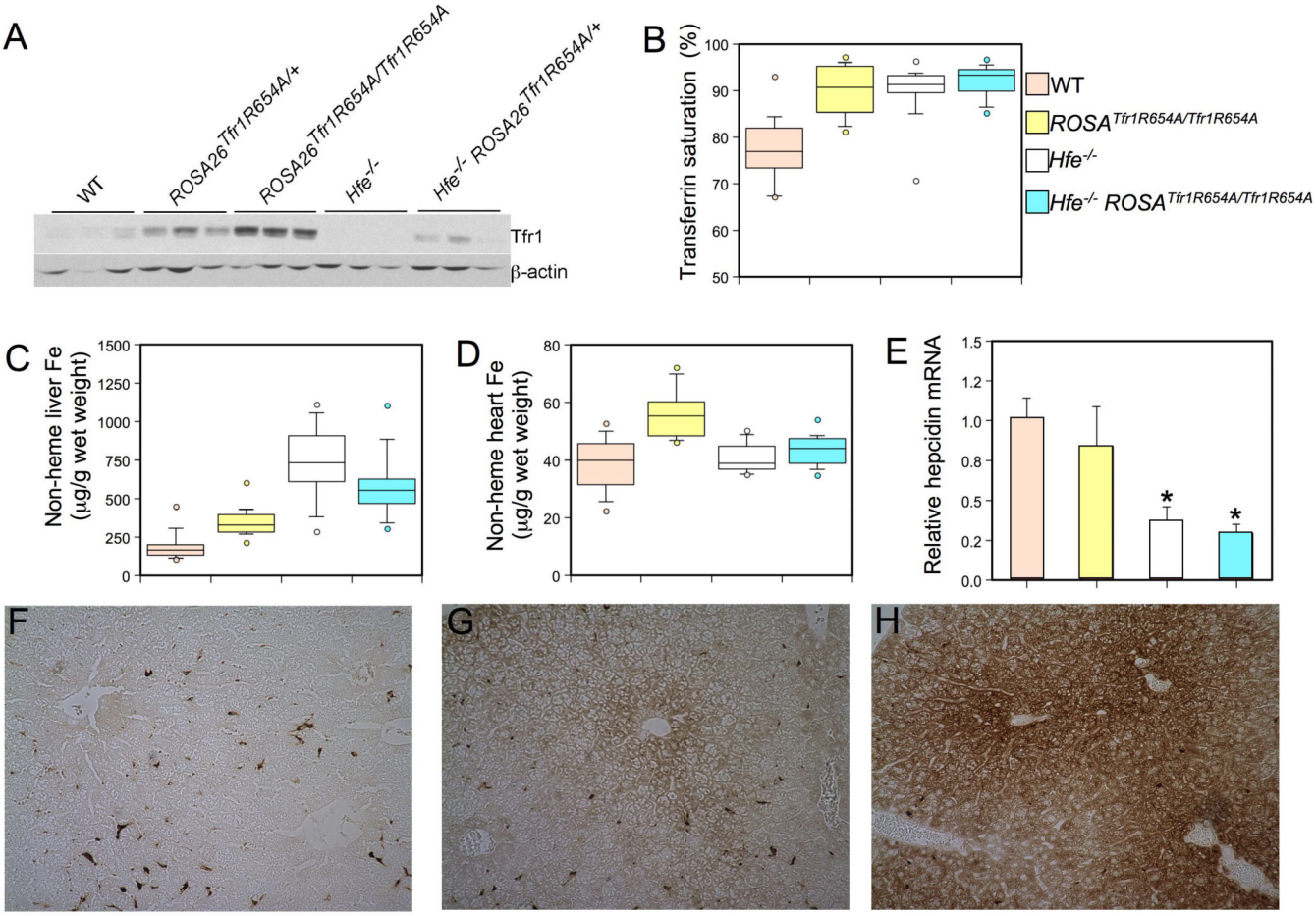


**Figure 2. Phenotypic analysis of *ROSA26$^{Tfr1R654A/Tfr1R654A}$* mice**

Tfr1 protein expression was analyzed (A, top panel) in wild type (WT), *ROSA26$^{Tfr1R654A/+}$*, *ROSA26$^{Tfr1R654A/Tfr1R654A}$*, *HFE$^{-/-}$*, and *HFE$^{-/-}$ ROSA26$^{Tfr1R654A/+}$* 8 week-old animals by western blot analysis. Equivalent loading of liver lysate was confirmed with immunoblot analysis (bottom panel) using an anti-β-actin antibody. Box plots depicting the measurement of (B) serum Tf saturation (%), (C) non-heme liver iron (µg/g wet weight), and (D) non-heme heart iron (µg/g wet weight). Wild type (WT, *n*=18, a), *ROSA26$^{Tfr1R654A/Tfr1R654A}$* (*n*=15, b), *Hfe$^{-/-}$* (*n*=17, c), *Hfe$^{-/-}$ ROSA26$^{Tfr1R654A/+}$* (*n*=13, d) are depicted in salmon, yellow, white and blue, respectively. The middle bar of the box represents the median, while the top of the box is the 75$^{th}$ percentile and the bottom of box is the 25$^{th}$ percentile. The top and bottom whiskers depict the 90$^{th}$ and 10$^{th}$ percentile of the data, respectively. Data outside of the 10$^{th}$ and 90$^{th}$ percentiles are drawn as circles. *P*-values were calculated with Microsoft Excel (Student's t-test). *P*-values: (B) a vs. b, c, or d *P*<0.001, (C) all groups *P*<0.005 except c vs. d *P*=NS, (D) *P*<0.001 a vs. b, b vs. c, b vs. d, *P*=NS all others. Total mRNA was harvested from *ROSA26$^{Tfr1R654A/Tfr1R654A}$* (E) livers (*n*=5, results expressed as mean ± SEM) and hepcidin mRNA was assessed by quantitative real-time PCR. Mean mRNA expression for wild type mice was set as 1 and all other data was expressed in relation to this. Significant differences in mRNA expression compared to WT are denoted (**P*<0.03). DAB-enhanced Perls stain (F, G and H) for iron in liver sections. Brown staining demonstrates iron accumulation in cells. Genotypes of mice are (F) wild type, (G) *ROSA26$^{Tfr1R654A/Tfr1R654A}$* and (H) *Hfe$^{-/-}$*.

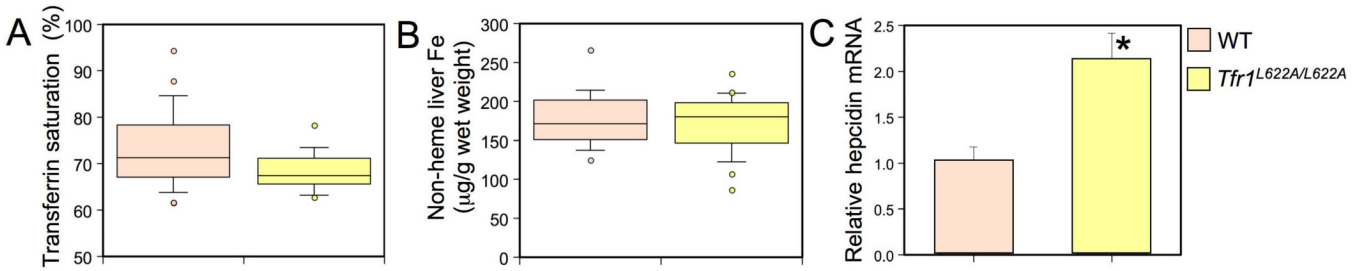


**Figure 3. Phenotypic analysis of *Tfr1*$^{L622A/L622A}$ mice**

Box plots depicting the measurement of (A) serum Tf saturation (%) and (B) non-heme liver iron (µg/g wet weight) as in Figure 2. Wild type (WT, *n*=21) and *Tfr1*$^{L622A/L622A}$ (*n*=16) are depicted in salmon and yellow, respectively. *P*-values: (A) *P*<0.02 and (B) *P*=NS. Liver hepcidin mRNA was analyzed (C) and graphed as in Figure 2. Significant differences in mRNA expression compared to WT are denoted (**P*<0.03).

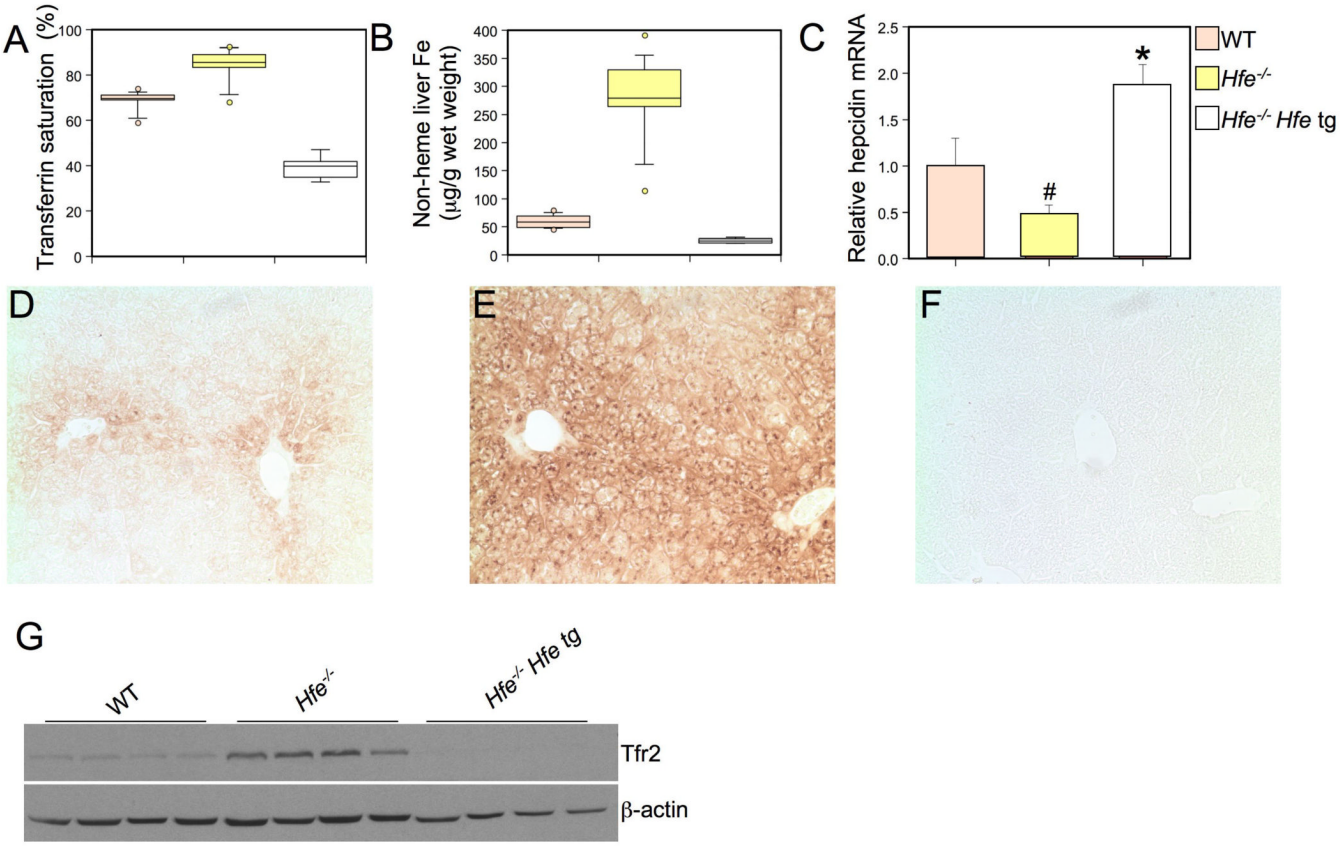


**Figure 4. Phenotypic analysis of mice expressing a hepatocyte-specific *Hfe* transgene (tg)**

Box plots depicting the measurement of (A) transferrin saturation (%) and (B) non-heme liver iron (µg/g wet weight) as in Figure 2. Wild type (WT, $n$=14, a), *Hfe*$^{-/-}$ ($n$=15, b), and *Hfe*$^{-/-}$ *Hfe* tg ($n$=7, c), are depicted in salmon, yellow, and white, respectively. $P$-values: (A) all groups $P<0.001$, (B) all groups $P<0.001$. Liver hepcidin mRNA was analyzed (C) and graphically represented as in Figure 2. Significant differences in mRNA expression are denoted (#$P<0.05$, *$P=0.03$). DAB-enhanced Perls stain (D, E and H) for iron in liver sections. Genotypes of mice are (D) wild type, (E) *Hfe*$^{-/-}$and (H) *Hfe*$^{-/-}$ *Hfe* tg. Tfr2 protein expression was analyzed (G, top panel) in wild type (WT), *Hfe*$^{-/-}$ and *HFE*$^{-/-}$ tg by western blot analysis. Equivalent loading of liver lysate was confirmed with immunoblot analysis (bottom panel) using an anti-β-actin antibody.

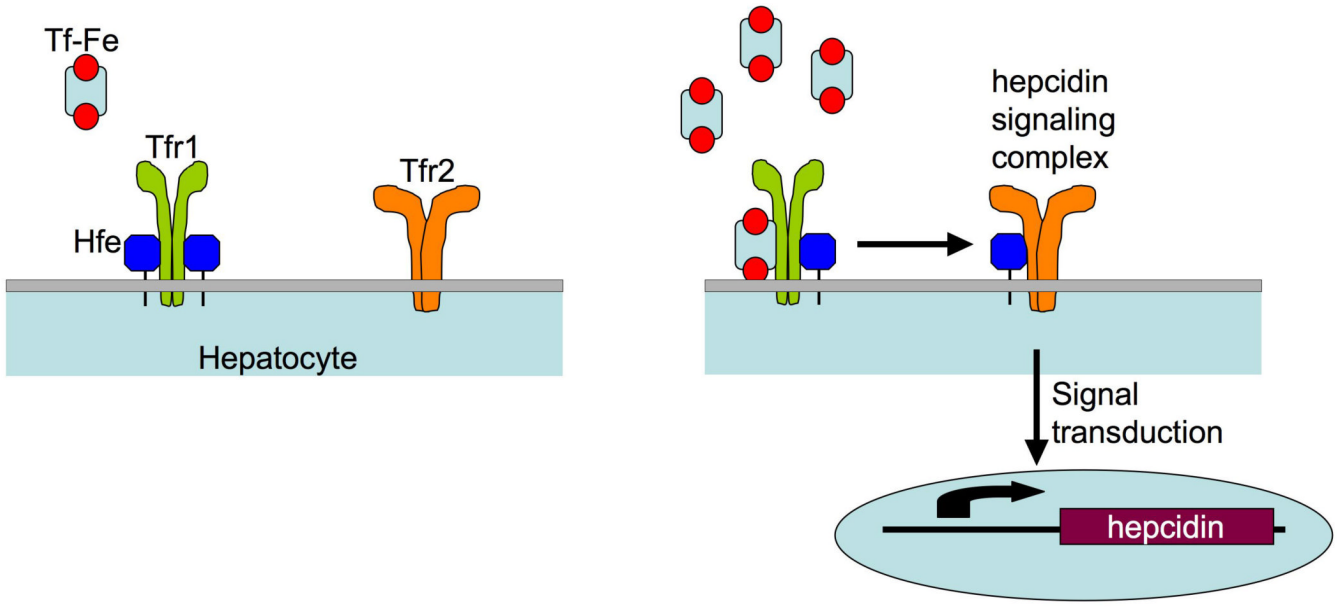


**Figure 5. Model for liver-centered serum iron sensing**

Hfe-Tfr1 complexes on the surface of hepatocytes sense the saturation of iron-bound transferrin in the serum. At low transferrin saturations, Hfe is sequestered by Tfr1 (left). As serum iron saturation increases, Hfe is dislodged from its overlapping binding site on Tfr1 by Fe-Tf (right). Hfe is then free to interact with Tfr2 and signal in some manner for the upregulation of hepcidin. Increased levels of circulating hepcidin lead to a reduction in both intestinal iron absorption and macrophage iron release. If either Hfe or Tfr2 is mutated or absent, the complex is unable to sense increased serum Tf saturation and dysregulation of iron homeostasis occurs.

**Table 1**

**Hematologic features of *Tfr1*$^{L622A/L622A}$ mice**

Red blood cell parameters were measured in 8 week-old female mice

| Genotype | Hgb (g/dl) | Hct (%) | MCV (fL) | MCH (pg) | RDW (%) | Retic (%) | CHr (pg) |
|---|---|---|---|---|---|---|---|
| WT (N=23) | 15.3 ± 0.2 | 50.9 ± 0.5 | 56.5 ± 0.3 | 17.0 ± 0.1 | 12.4 ± 0.1 | 5.1 ± 0.4 | 16.4 ± 0.1 |
| *Tfr1*$^{L622A/L622A}$ (N=15) | 14.5 ± 0.2 | 45.8 ± 0.4 | 50.3 ± 0.3 | 15.9 ± 0.1 | 13.8 ± 0.1 | 5.2 ± 0.3 | 16.4 ± 0.1 |
| *P, WT* vs *Tfr1*$^{L622A/L622A}$ | *P*<0.001 | *P*<0.001 | *P*<0.001 | P<0.001 | *P*<0.001 | *P*=NS | *P*=NS |

WT = wild type; NS = not significant. The measured parameters were hemoglobin (Hgb), hematocrit (Hct), mean cell volume (MCV), mean cell hemoglobin (MCH), red cell distribution width (RDW), reticulocyte count (Retic), and reticulocyte mean cell hemoglobin (CHr). Values are mean ± SEM. *P*-values (Student's T-test) were calculated using Microsoft Excel.

**Table 2**

**Hematologic features of *Hfe*$^{-/-}$ *Hfe* tg animals**

Red blood cell parameters were measured in 8 week-old female mice

| Genotype | Hgb (g/dl) | Hct (%) | MCV (fL) | MCH (pg) | RDW (%) | Retic (%) | CHr (pg) |
|---|---|---|---|---|---|---|---|
| WT (N=12) | 14.7 ± 0.1 | 46.8 ± 0.4 | 49.6 ± 0.3 | 15.6 ± 0.1 | 13.4 ± 0.2 | 3.6 ± 0.2 | 16.3 ± 0.1 |
| *Hfe*$^{-/-}$ (N=14) | 15.6 ± 0.2 | 50.6 ± 0.8 | 52.6 ± 0.6 | 16.3 ± 0.1 | 13.1 ± 0.2 | 3.6 ± 0.2 | 16.2 ± 0.7 |
| *Hfe*$^{-/-}$ *Hfe* tg (N=6) | 12 ± 0.3 | 39.9 ± 0.8 | 38.2 ± 0.6 | 11.5 ± 0.1 | 22.2 ± 0.7 | 4.5 ± 0.4 | 12.8 ± 0.2 |
| *P*, *Hfe*$^{-/-}$ vs *Hfe*$^{-/-}$ *Hfe* tg | *P*<0.001 | *P*<0.001 | *P*<0.001 | *P*<0.001 | *P*<0.001 | NS | *P*<0.001 |
| *P*, WT vs *Hfe*$^{-/-}$ *Hfe* tg | *P*<0.001 | *P*<0.001 | *P*<0.001 | *P*<0.001 | *P*<0.001 | NS | *P*<0.001 |
| *P*, WT vs *Hfe*$^{-/-}$ | *P*<0.001 | *P*<0.001 | *P*<0.001 | *P*<0.001 | NS | NS | NS |

WT = wild type; NS = not significant, tg = transgene. The measured parameters were hemoglobin (Hgb), hematocrit (Hct), mean cell volume (MCV), mean cell hemoglobin (MCH), red cell distribution width (RDW), reticulocyte count (Retic), and reticulocyte mean cell hemoglobin (CHr). Values are mean ± SEM. *P*-values (Student's T-test) were calculated using Microsoft Excel.